Available online at www.sciencedirect.com
SCIENCE DIRECT
Solid State Communications 137 (2006) 483–487
solid state communications
www.elsevier.com/locate/ssc

# Effect of $OH^-$ on the upconversion luminescent efficiency of $Y_2O_3$:$Yb^{3+}$, $Er^{3+}$ nanostructures

Gejihu De [a,b], Weiping Qin [a,c,*], Jisen Zhang [a,c], Jishuang Zhang [a,b], Yan Wang [a,b], Chunyan Cao [a,b], Yang Cui [a,b]

[a] *Key Laboratory of Excited State Processes, Changchun Institute of Optics, Fine Mechanics and Physics, Chinese Academy of Science, 16 East Nanhu Road, Changchun 130033, China*
[b] *Graduate School of Chinese Academy of Sciences, Beijing 100039, China*
[c] *State Key Laboratory of Integrated Optoelectronics, College of Electronic Science and Engineering, Jilin University, Changchun 130012, China*

Received 27 May 2005; received in revised form 1 December 2005; accepted 27 December 2005 by B. Jusserand
Available online 23 January 2006

**Abstract**

In this work, we used the hydrothermal method to synthesize $Yb^{3+}$ and $Er^{3+}$ ions doped cubic $Y_2O_3$ nanostructures, which is an upconversion luminescent material. Three distinct shapes such as nanotubes, nanospheres and nanoflakes formed in the products by adjusting the pH value of reacting solution. Powder X-ray diffraction analyses indicate that all the three nanostructures were pure cubic phase, while electron microscopy measurements confirm the formation of different morphologies. These nanostructures exhibit strong visible upconversion luminescence under the excitation of a 978-nm diode laser. The FTIR and fluorescent decay measurements at the size and morphology of sample changed from tubes to flakes indicate that the $OH^-$ group is the origin of luminescent efficiency change. $OH^-$ ions with high vibration frequency provide an efficient means to quench the luminescence. However, the relative intensity and pump-power dependence of the green and red emissions varies with the three nanostructures possessing different size and morphology.


*PACS:* 73.63.Bd; 78.55.-m; 78.67.Bf; 74.62.Dh

*Keywords:* A. $Y_2O_3$ nanostructures; C. Scanning and transmission electron microscopy; E. Luminescence, size and morphology

## 1. Introduction

Rare earth ion-doped inorganic nanostructure materials have attracted much attention in recent years because of their unique properties and potential applications in functional nanodevices [1–3]. It is generally accepted that these nanostructures provide an ideal system to investigate the dependence of electrical, optical, and mechanical properties on size and dimensionality. Rare earth (RE) compounds have been demonstrated in a wide range application such as high-performance magnets, luminescence materials and catalysts, and most of these functions depend strongly on the size and structure. $Y_2O_3$ doped with $RE^{3+}$ is phosphors extensively used in optical display and light emitting devices. The trend towards nanoscale science has raised interests in preparation of various $Y_2O_3$ nanostructures. In our previous report [4], $Y_2O_3$:Eu nanotubes were fabricated by surfactant self-assembly and their optical properties were investigated using laser selective spectroscopy. Recently, Yadong Li et al. reported the synthesis of RE nanotubes by a facile hydrothermal method, and their nanotubes have small inner diameters of 10 nm and single thin inorganic walls of about 1 nm [5,6]. Other type of $Y_2O_3$ structures such as nanoparticles and thin films have also been investigated extensively in order to develop high efficient phosphors for light-emitting devices [7,8].

There is a growing interest in conversion of infrared radiation into shorter wavelengths by the materials doped with RE ions. $Er^{3+}$ ion is an ideal candidate for this purpose due to its versatile energy levels in the near infrared region. Codoping of $Yb^{3+}$ ion as a sensitizer can yield a substantial improvement in upconversion efficiency due to the efficient energy transfer between the sensitizer and the emitter [9–11]. The availability of high-power infrared laser diodes has stimulated researchers

* Corresponding author. Address: Key Laboratory of Excited State Processes, Changchun Institute of Optics, Fine Mechanics and Physics, Chinese Academy of Science, 16 East Nanhu Road, Changchun 130033, China. Tel.: +86 431 6176352; fax: +86 431 4627031.
*E-mail address:* wpqin@public.cc.jl.cn (W. Qin).

0038-1098/$ - see front matter © 2006 Elsevier Ltd. All rights reserved.
doi:10.1016/j.ssc.2005.12.034

to develop near infrared to visible upconversion lasers, light-emitting devices and three-dimensional displays [12–14]. Furthermore, the upconverting phosphors have been used to enhance the near-infrared response of silicon solar cell [15]. Meanwhile, RE-doped nanocrystals have also been demonstrated to be promising upconversion fluorescence labels in biological detections [16]. In this letter, the dependence of upconversion luminescence in $Er^{3+}/Yb^{3+}$ copoped $Y_2O_3$ nanostructures on morphology was reported.

## 2. Experimental

The method for fabricating $Y_2O_3$:$Yb^{3+}$,$Er^{3+}$ nanotubes is as follows: in a typical synthesis, 0.94 mmol $Y_2O_3$ (Aldrich), 0.04 mmol $Yb_2O_3$ (Aldrich) and 0.02 mmol $Er_2O_3$ (Aldrich) were dissolved in nitric acid (Aldrich 63%) to form clear aqueous solution, then 10% KOH solution was added to adjust the system to pH is about 6.0. The as-obtained colloidal precipitate was transferred into a 25 mL autoclave, sealed and kept at 160 °C for 3 days. After that, the autoclave was allowed to cool to room temperature naturally. The precipitate was then centrifuged, washed with deionized water to remove impurity ions in the final products, and dried at 200 °C in air. The resulting solid was put into a furnace. The furnace temperature was gradually raised to 500 °C (in air) and kept for 4 h. The synthesis of nanospheres and nanoflakes is similar to that of the nanotubes, but adjust the pH value of the reacting solution to be 6.5 and 7.0, respectively.

The crystal structures were analyzed by a Rigaku RU-200b X-ray powder diffractometer with Cu $K_\alpha$ radiation ($\lambda = 0.15406$ nm). The size and morphology were investigated by scanning transmission microscopy (SEM, KYKY 1000B) and transmission electron microscope (TEM, JEM 2010 with operating voltage of 200 kV). The upconversion luminescence spectra were recorded with a Hitachi F-4500 fluorescence spectrophotometer under the 978-nm excitation.

Infrared spectra of powders (FTIR) were recorded in the range of 1500–4000 $cm^{-1}$ on a Fourier transform spectrometer (Perkin–Elmer, Spectrum 1, USA) with a resolution of 1 $cm^{-1}$. The powder samples were mixed with KBr then pressed into a cylindrical die.

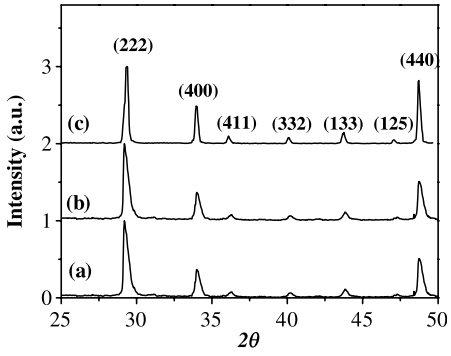


Fig. 1. XRD patterns of $Y_2O_3$:Yb,Er nanostructures: (a) nanotubes, (b) nanospheres, and (c) nanoflakes.

## 3. Results and discussion

The XRD patterns of the $Y_2O_3$:$Yb^{3+}$,$Er^{3+}$ nanostructures were presented in Fig. 1, where (a), (b), and (c) curves correspond to nanotubes, nanospheres, and nanoflakes, respectively. The three samples exhibit identical patterns although they possess different morphologies. All the diffraction peaks can be readily indexed to a pure cubic phase [space group $Ia\bar{3}(206)$] with lattice constant $a = 10.55$ nm, which is in good agreement with the standard values for the bulk cubic $Y_2O_3$ (JCPDS 74-1828). No other impurities have been found in the synthesized products.

Fig. 2(a) gives the TEM images of $Y_2O_3$:$Yb^{3+}$,$Er^{3+}$ nanotubes. As can be seen, the central part of the cylindrical sample is white and the two peripheries are black, suggesting the formation of nanotubes. A bundle aggregate of nanotubes is also observed in the TEM image. The nanotubes appear to have a diameter of ~30 nm and a length up to several micrometers. The walls of nanotubes are estimated to be ~5 nm in thickness. The inset shows the electron diffraction pattern recorded perpendicularly to the nanotube long axis, which reveals that the nanotubes are single crystalline, and also stable enough to withstand the irradiation of convergent high-energy electron beam. Fig. 2(b) and (c) show the SEM images of $Y_2O_3$:$Yb^{3+}$,$Er^{3+}$ nanospheres and nanoflakes, respectively. The nanospheres are relatively uniform, with an average diameter of ~90 nm. Some cross sections of the nanoflakes can be observed in Fig. 2(c), from which the thickness of the nanoflakes is estimated to be ~50 nm. However, they are not uniform in the lateral size, varying from half a micrometer to one micrometer.

$Yb^{3+}$ sensitized $Er^{3+}$ ion is an efficient system for near-infrared to visible frequency upconversion. For $Y_2O_3$:-$Yb^{3+}$,$Er^{3+}$ nanostructures in this study, bright visible luminescence can be clearly observed with naked eyes under relative weak 980-nm excitation, which promised efficient upconversion nanophosphors. In $Yb^{3+}/Er^{3+}$ codoped materials, upconverted emission may result from different processes, including multi-step excited state absorption (ESA), energy transfer (ET) between neighboring excited $Er^{3+}$ ions, and APTE (addition de photons par transfer d' Energie) between $Yb^{3+}$ and $Er^{3+}$ ions, among which APTE is the most efficient [17]. Fig. 3 shows the energy levels and upconversion mechanism in $Yb^{3+}/Er^{3+}$ codoped system. A 978-nm photon excites an $Yb^{3+}$ ion from the ground state $^2F_{7/2}$ to the excited state $^2F_{5/2}$, which may transfer the energy to a nearby $Er^{3+}$ ion, promoting the $Er^{3+}$ ion from $^4I_{15/2}$ to the $^4I_{11/2}$ state, and if the latter is already populated, the $Er^{3+}$ ion may transit from the $^4I_{11/2}$ to the $^4F_{7/2}$ states. Subsequent nonradiative relaxations could populate the $^2H_{11/2}$ and $^4S_{3/2}$ states that are the emitting levels for the green luminescence. The $^4I_{11/2}$ states of $Er^{3+}$ ions could be depopulated by an alternative relaxation route to $^4I_{13/2}$ states, which may be further excited to the red-emitting levels $^4F_{9/2}$, and the corresponding transition to the ground state $^4I_{15/2}$ produces red emission.

In Fig. 4(a), the top curve represents the room temperature upconversion emission spectrum of the $Y_2O_3$: $Yb^{3+}$,$Er^{3+}$

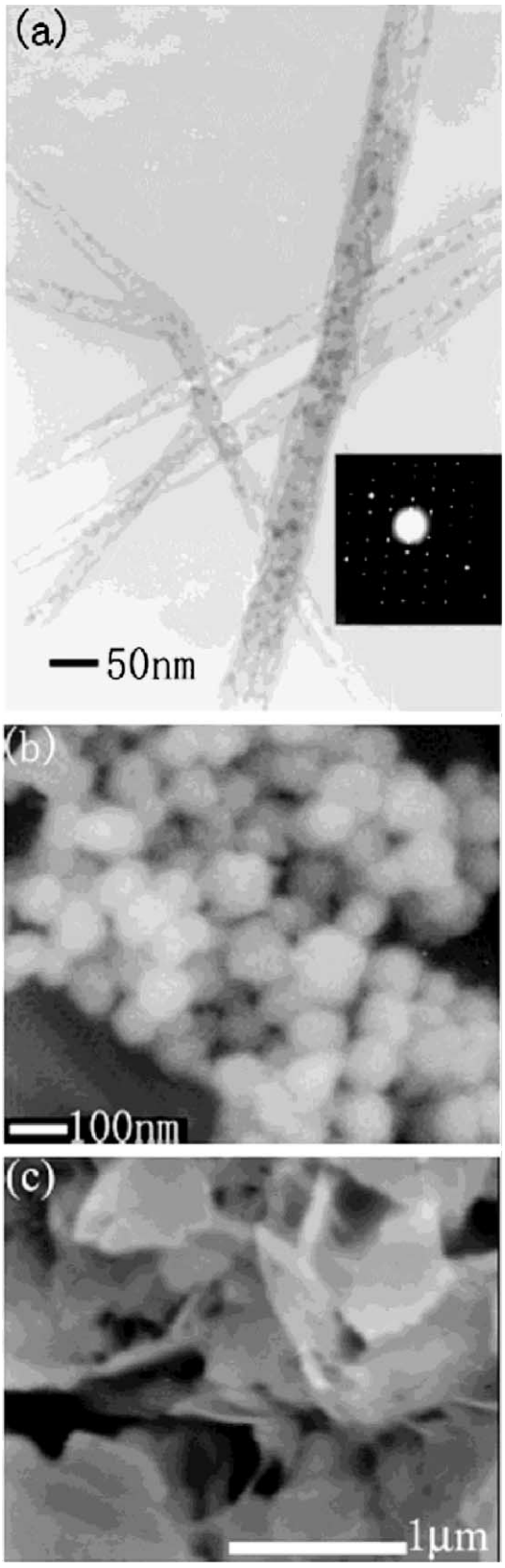


Fig. 2. (a) TEM image of $Y_2O_3$:Yb,Er nanotubes, the inset shows the electron diffraction pattern; (b) SEM image of $Y_2O_3$:Yb,Er nanospheres; (c) SEM image of $Y_2O_3$:Yb,Er nanoflakes.

nanotubes, where the red emission around 650 nm can be clearly observed and the green emission is very weak. The upconversion emission spectra of $Y_2O_3$:$Yb^{3+}$,$Er^{3+}$ nanospheres and nanoflakes are also illustrated in Fig. 4(a). The spectra exhibit three distinct emission bands around 408, 520–570 and 650–670 nm, which correspond to the transitions $^2H_{9/2}\rightarrow{}^4I_{15/2}$ (blue emission), $^2H_{11/2}$, $^4S_{3/2}\rightarrow{}^4I_{15/2}$ (green emission), $^4F_{9/2}\rightarrow{}^4I_{15/2}$ (red emission), respectively. A significant feature of these spectra is that the relative intensity of upconversion emissions varies with the nanostructures of different morphologies. According to Fig. 4(a), the intensity ratios of green emission to red emission are estimated to be 0.09, 0.33, and 0.87 for the nanotubes, nanospheres and nanoflakes, respectively. Where, the integrated areas of peaks are used to calculate the emission intensities. Such spectral change may result from several factors such as host composition [18] and doped concentration [19]. Basically, the host composition determines the phonon energy, thus the multi-phonon relaxation rate, while different doped concentrations affect the distance between the active ions, leading to the changes in energy transfer rate and cross relaxation rate. However, in our case the three nanostructures were prepared through the similar hydrothermal method and the reaction systems were designed to have the same concentration of $Yb^{3+}$ and $Er^{3+}$ ions. Particularly, the pH value was adjusted very slowly under vigorous stirring so that the active ions were uniformly dispersed in the materials. Furthermore, XRD analysis has confirmed that all the three nanostructures possess cubic structure with the same lattice constant. Therefore, another effect, rather than the host composition and the doped concentration, should be considered to clarify the spectral differences among the three nanostructures.

Dependence of the upconversion luminescence intensity on pump-power was performed to obtain a better understanding of the upconversion processes. For unsaturated upconversion luminescence, the emission intensity, $I_{em}$, is proportional to $I_{ex}^n$, where $I_{ex}$ is the excitation intensity and the integer $n$ is the order of upconversion process. More specifically, $n$ is the number of pump photons required to populate the emitting

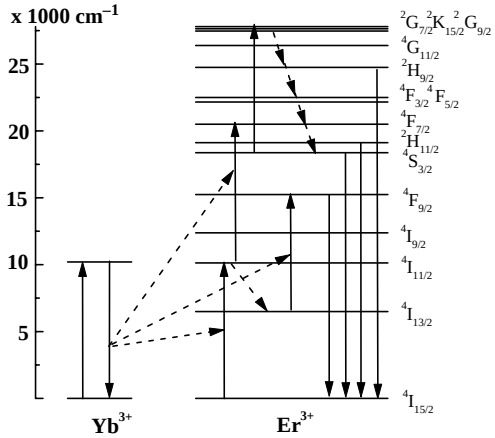


Fig. 3. Schematic diagram of $Yb^{3+}$ sensitized $Er^{3+}$ upconversion luminescence under 978-nm excitation.

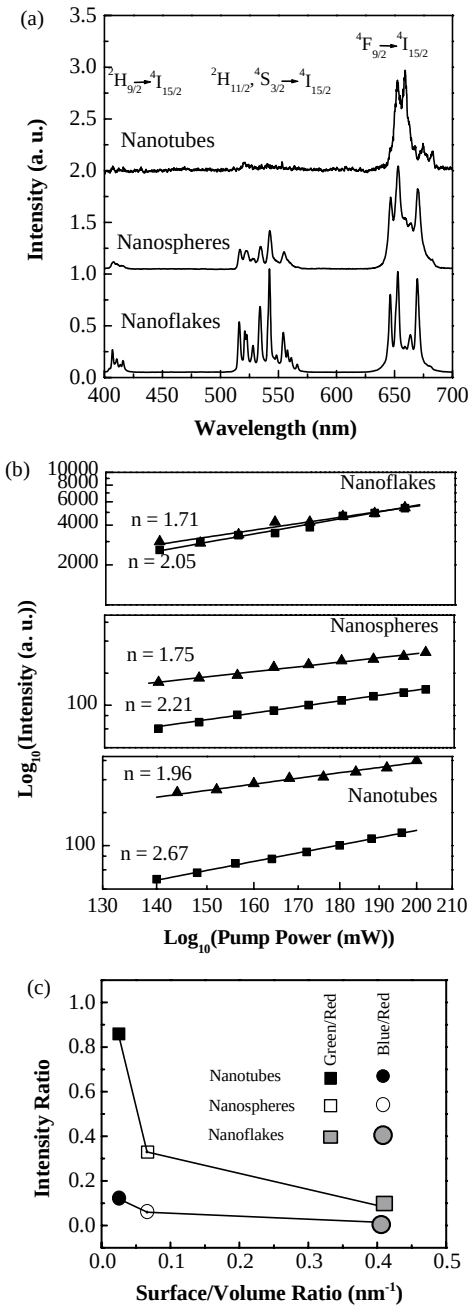


Fig. 4. (a) Room-temperature upconversion emission spectra of $Y_2O_3$:Yb,Er nanotubes, nanospheres, and nanoflakes; (b) log–log plot of upconversion intensity versus pump-power in $Y_2O_3$:Yb,Er nanostructures. Uptriangles (▲) represent red emissions and squares (■) indicate green emissions; (c) the intensity ratio of green/blue to red emissions as a function of the surface to volume ratio in the three nanostructures. The green to red emission ratios are indicated by square while the blue to red ratios are illustrated using circle symbols.

state, which can be determined from the slope of log–log plot of upconversion intensity versus pump-power [20]. Fig. 4(b) shows the excitation dependence of the green (■) and red (▲) upconversion emissions for the $Y_2O_3$:$Yb^{3+}$,$Er^{3+}$ nanostructures, where the fitting of the data yields straight lines and the values of the slopes are also listed. As can be seen, there is a gradual increase in the slope for both green and red emission while the material changes from large-sized nanoflakes to small-sized nanotubes. Particularly, the green emission of the nanotubes produces a slope value of 2.67, which means that three-photon process may be partially involved in the green emission. According to Fig. 3, three-photon process generally populates the energy states ($^2G_{7/2}$, $^2K_{15/2}$, $^2G_{9/2}$). However, a fast cascade relaxation from these states to green-emitting levels may occur if there is a strong coupling between $Er^{3+}$ ions and $OH^-$ groups adsorbed on the nanotubes. Therefore, it is reasonable that the three-photon process practically leads to green emission in a typical material system with high-energy vibrations. On the other hand, the increase in the slope from nanoflakes to nanotubes further confirms that the presence of surface groups ($OH^-$) do have a great influence on the upconversion luminescence of the $Y_2O_3$:$Yb^{3+}$,$Er^{3+}$ nanostructures.

When the material size approaches nanoscale, some energy states related to surfaces and interfaces appear to play an important role in determining the optical properties of RE related luminescent materials [4,21]. Generally, such surface states was closely related with some anionic groups such as $OH^-$ which originate from the precursors in the synthesis and cannot be removed even through a long time heat treatment [22,23]. In our case, the nanostructures were prepared by the hydrothermal method. It is reasonable to conclude that there has certain amount of $OH^-$ ions adsorbed on the surface. The $OH^-$ group yields high-energy vibrational modes (3200–3600 $cm^{-1}$), compared to the intrinsic phonons of $Y_2O_3$ with a cutoff of phonon energy 597 $cm^{-1}$ [23]. These high-energy vibrations would strongly quench the excited states of $Er^{3+}$ ions by multi-phonon relaxation, thus leading to a great influence on the upconversion processes. The multi-phonon relaxation rate, $W_p$, which can be expressed by the Miyakawa–Dexter equation [24],

$$W_p = W_p(0)\exp\left(\frac{-\alpha\Delta E}{\hbar\omega}\right) \tag{1}$$

$$\alpha = \ln\left\{\frac{p}{g[n(t)+1]}\right\} - 1$$

$$p \approx \frac{\Delta E}{\hbar\omega}$$

where $g$ is the electron–phonon coupling strength, $\Delta E$ is the energy gap to the next lower level, $\hbar\omega$ is the phonon energy and the $p$ is phonon numbers needed in the multi-phonon relaxation. For $Er^{3+}$ ions, the $^4I_{11/2}$ and $^4I_{13/2}$ states are the intermediate levels responsible for green and red emissions, respectively. There is an energy gap of ~3600 $cm^{-1}$ between the two states. According to Eq. (1), the high-energy vibrations from $OH^-$ groups makes the multi-phonon relaxation ($^4I_{11/2}\rightarrow{}^4I_{13/2}$) much more probable than that of the intrinsic phonons in bulk $Y_2O_3$, where at least six phonons are required to bridge the gap. As is well known, the upconversion intensity depends on the population of the intermediate states. Therefore, the presence of $OH^{-1}$ groups

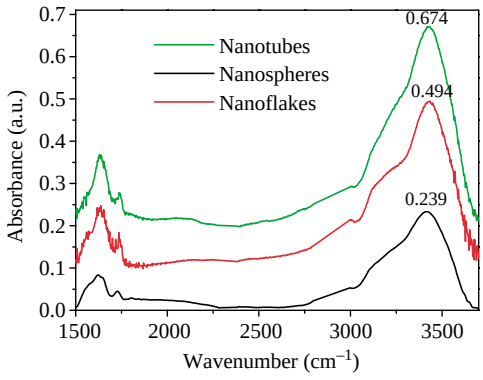


Fig. 5. FTIR spectra of samples (a) nanotubes, (b) nanospheres, and (c) nanoflakes.

on the surface would result in an enhanced red emission and reduced green emission if they are coupled with $Er^{3+}$ ions. To further clarify this effect, a relationship between upconversion emissions and $Y_2O_3$:$Yb^{3+}$,$Er^{3+}$ nanostructures with different shapes was established. Here the ratio of surface area to volume is used to describe the three nanostructures since the materials have different dimensions and the size and morphology are correlated. According to the images in Fig. 2, the ratios of surface area to volume were estimated to be 0.400, 0.066, and 0.025 $nm^{-1}$ for the nanotubes, nanospheres, and nanoflakes, respectively. The line-squares in Fig. 4(c) present the intensity ratio of green to red emissions as a function of the surface to volume ratio in the three nanostructures. As is shown, with the surface to volume ratio increasing, there would be more and more $Er^{3+}$ ions located near the surfaces, resulting in a stronger coupling between $Er^{3+}$ and $OH^-$. Consequently, the green upconversion emission decreases compared to the red one, as the morphology changes from large-sized nanoflakes to small-sized nanotubes. Similar tread were also observed for the blue to red emission ratios, as illustrated by the line-circles in Fig. 4(c). Obviously, the presence of $OH^-$ ions has similar quenching effect on the higher excited states that are responsible for the blue upconversion emissions.

Fig. 5 presents the FTIR spectrum of samples (a) nanotubes, (b) nanospheres and (c) nanoflakes. The peaks at about 1623 and a broad band ranging from 2750 to 3700 $cm^{-1}$ are characteristic of the vibration of $OH^-$ groups. The vibration intensity of OH group decreases markedly as the morphology of sample changes from tubes to films. In fact, $OH^-$ ions are adsorbed into the host surface easily due to the nature of the wet-chemical route. $OH^-$ ions originate from two aspects: on one hand, the synthesis was conducted in the aqueous solution, and thus $OH^-$ ions came from $H_2O$; on the other hand, the sample was annealed in air, and thus $OH^-$ ions came from air.

## 4. Conclusion

$Y_2O_3$:$Yb^{3+}$,$Er^{3+}$ nanostructures with different shapes, nanotubes, nanospheres and nanoflakes, were synthesized by adjusting the pH value of reacting solution in a hydrothermal method. Powder X-ray diffraction analysis indicates that all the three nanostructures are pure cubic phase, while SEM and TEM measurements confirm the formation of different morphologies. The samples present strong visible upconversion luminescence with the excitation of a 978-nm diode laser. It is suggested that the $OH^-$ groups adsorbed on the sample surface have a significant influence on the upconversion processes, leading to the variances in the relative intensity and pump-power dependence of the green and red emissions.

## Acknowledgements

The authors would like to thank the support of the National Science Foundation of China (Grant No. 10274082 and No. 10474096).

## References

[1] X. Peng, L. Manna, W. Yang, J. Wickham, E. Scher, A.P. Kadavanich, A. Alivisatos, Nature 404 (2000) 59–61.
[2] Y. Xia, P. Yang, Y. Sun, Y. Wu, B. Mayers, B. Gates, Y. Yin, F. Kim, H. Yan, Adv. Mater. 15 (2003) 353–389.
[3] Q. Song, Z. Zhang, J. Am. Chem. Soc. 126 (2004) 6164–6168.
[4] C. Wu, W. Qin, G. Qin, D. Zhao, J. Zhang, S. Huang, S. Lu, H. Liu, H. Lin, Appl. Phys. Lett. 82 (2003) 520–522.
[5] X. Wang, Y. Li, Angew. Chem. Int. Ed 41 (2002) 4790–4793.
[6] X. Wang, X. Sun, D. Yu, B. Zou, Y. Li, Adv. Mater. 15 (2003) 1442–1445.
[7] G. Wakefield, E. Holland, P.J. Dobson, J.L. Hutchison, Adv. Mater. 13 (2001) 1557–1560.
[8] D. Kumar, J. Sankar, K. Cho, G.V. Craciun, R.K. Singh, Appl. Phys. Lett. 77 (2000) 2518–2520.
[9] G. Qin, W. Qin, S. Huang, C. Wu, D. Zhao, B. Chen, S. Lu, S. E, J. Appl. Phys. 92 (2002) 6936–6938.
[10] G. Qin, W. Qin, C. Wu, S. Huang, J. Zhang, S. Lu, D. Zhao, H. Liu, J. Appl. Phys. 93 (2003) 4328–4330.
[11] F. Vetrone, J.C. Boyer, J.A. Capobianco, A. Speghini, M. Bettinelli, J. Phys. Chem. B 107 (2003) 1107–1112.
[12] G. Qin, W. Qin, C. Wu, S. Huang, D. Zhao, Z.J. Zhao, S. Lu, Opt. Commun. 242 (2004) 215–219.
[13] D. Matsuura, Appl. Phys. Lett. 81 (2002) 4526–4528.
[14] E. Downing, L. Hesselink, J. Ralston, R. Macfarlane, Science 273 (1996) 1185–1189.
[15] A. Shalav, B.S. Richards, T. Trupke, K.W. Krämer, H.U. Güdel, Appl. Phys. Lett. 86 (1–3) (2005) 013505.
[16] G. Yi, H. Lu, S. Zhao, Y. Ge, W. Yang, D. Chen, L. Guo, Nano Lett. 4 (2004) 2191–2196.
[17] F. Auzel, Chem. Rev. 104 (2004) 139–173.
[18] J. Yang, L. Zhang, L. Wen, S. Dai, L. Hu, Z. Jiang, J. Appl. Phys. 95 (2004) 3020–3026.
[19] F. Vetrone, J. Boyer, J.A. Capobianco, A. Speghini, M. Bettinelli, Chem. Mater. 15 (2003) 2737–2743.
[20] M. Pollnau, D.R. Gamelin, S.R. Lüthi, H.U. Güdel, M.P. Hehlen, Phys. Rev. B 61 (2000) 3337–3346.
[21] R.S. Meltzer, W.M. Yen, H. Zheng, S.P. Feofilov, A.F. Ioffe, M.J. Dejneka, Phys. Rev. B 66 (2002) 224202–224207.
[22] J.A. Capobianco, V. Fiorenzo, J.C. Boyer, J. Phys. Chem. B 106 (2002) 1181–1187.
[23] J.A. Capobianco, F. Vetrone, T. DoeAlesio, G. Tessari, A. Speghini, M. Bettinelli, Phys. Chem. Chem. Phys. 2 (2000) 3203–3207.
[24] T. Miyakawa, D.L. Dexter, Phys. Rev. B 1 (1970) 2961–2969.